VERSITA

OPTO-ELECTRONICS REVIEW **21**(4), 402–405

DOI: 10.2478/s11772-013-0101-y

High-operating temperature MWIR nBn HgCdTe detector grown by MOCVD

M. KOPYTKO*[1], A. KĘBŁOWSKI[2], W. GAWRON[1], P. MADEJCZYK[1], A. KOWALEWSKI[1], and K. JÓŹWIKOWSKI[1]

[1]Institute of Applied Physics, Military University of Technology, 2 Kaliskiego St., 00–908 Warsaw, Poland
[2]Vigo System S.A., 129/133 Poznańska St., 05–850 Ożarów Mazowiecki, Poland

The paper reports on the first experimental results of the mid-wave infrared (MWIR) HgCdTe barrier detectors operated at near-room temperatures and fabricated using metal organic chemical vapor deposition (MOCVD). SIMS profiles let to compare projected and obtained structures and reveals interdiffusion processes between the layers. Undesirable iodine diffusion from cap to the barrier increase the valance band offset and is the key item in limiting the performance of HgCdTe nBn detector. However, MOCVD technology with a wide range of composition and donor/acceptor doping and without post grown annealing might be successfully adopted for barrier device architectures.

Keywords: MOCVD growth, HgCdTe photodetectors, barrier photodetectors, uncooled photodetectors, Auger suppression.

1. Introduction

The development of technology for HgCdTe heterostructures with sophisticated composition and doping profiles enables a design of infrared detectors achieving BLIP performance at near-room temperatures [1–5]. Nowadays, one of the leading research topics in the world in HgCdTe heterostructure materials are nBn type detectors presenting technological advantages over p-on-n HgCdTe photodiodes. The nBn detector structure uses a unipolar barrier to suppress dark current and noises without impending photocurrent flow. The introduction of the wide bandgap barrier layer causes those Shockley-Read-Hall (SRH) generation-recombination (G-R) processes, as well as, surface leakage current is suppressed [6]. Despite the fact that $A_{III}B_V$ family compounds play dominant role in designing of the barrier detectors, due to nearly zero band-offset in valance band [7,8], the nBn architecture was successfully adapted to HgCdTe alloy in a molecular beam epitaxy (MBE) for long, as well as, medium range of infrared spectrum [9–11]. Due to the high content of the HgTe compound in a narrow bandgap HgCdTe material and, hence a large interdiffusion of mercury with a relatively high temperature of the MOCVD process, obtaining of sophisticated heterostructures with sharp and well-controlled gradients of composition and doping required for fabrication of long wavelength infrared (LWIR) barrier detectors is difficult. However, the MOCVD technique might be promising for MWIR barrier detectors.

Currently, the nBn architecture has been implemented successfully in the HgCdTe MBE growth. The very first experimental results related to the MWIR nBn type HgCdTe detectors were presented by Velicu *et al.* [9]. The uniform n-type doping of HgCdTe material is well controlled in MBE method; however, controllable *p*-type doping requires inconvenient *ex-situ* As-activation after implantation process. For that reason MOCVD growth seems to be more attractive because it allows to obtain *in-situ*, both donor and acceptor doping. Thus it is possible to grow both *n*- and *p*-type of the barrier. Proper *p*-type doping of the barrier allows reduction of the valence band offset which is the key item in limiting the performance of HgCdTe nBn detector.

This paper present the experimental results of the electrical and optical characteristics of MOCVD grown high-operating temperature MWIR HgCdTe nBn detectors with *n*- and *p*-type barriers.

2. Epitaxial growth and processing

The MWIR nBn HgCdTe structure was grown in Aixtron AIX-200 MOCVD system. The high operation temperature (HOT) barrier detector architecture consists of four layers. At the bottom, on a 3-μm thick CdTe buffer layer, the 5-μm thick highly *n*-type doped with iodine ($N_D = 1 \times 10^{17}$ cm^{-3}) wider-gap ($x = x_{abs} + 0.1$) contact layer was formed. Then, an undoped absorber was grown with a thickness of 3 μm and composition $x_{abs} = 0.36$. The donor background concentration of the material is about $N_D = (3 \div 6) \times 10^{15}$ cm^{-3}. On the absorbing layer, a thick (0.25 and 0.5 μm) undoped or *p*-type doped with arsenic ($N_A = 7 \times 10^{15}$ cm^{-3}) barrier with

*e-mail: mkopytko@wat.edu.pl

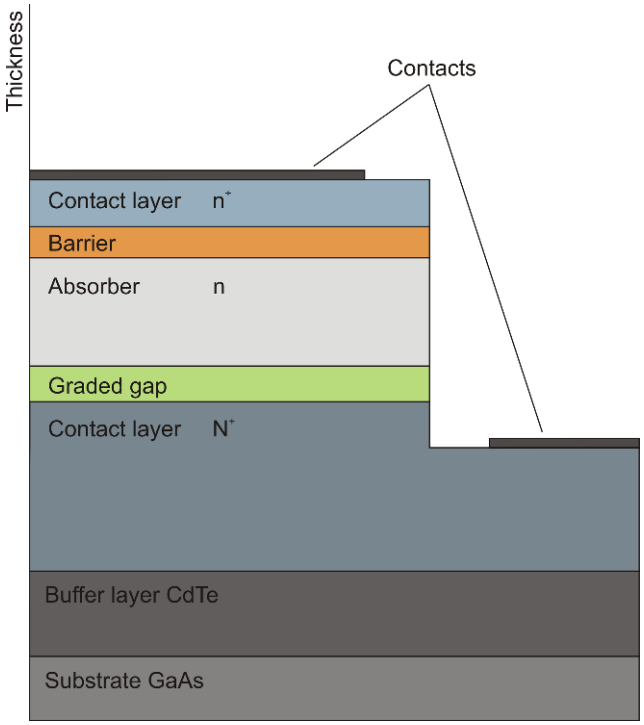

Fig. 1. Cross-section of mesa structure of MWIR HgCdTe nBn photodetector.

a composition $x_B = 1$ was formed. In our experiments the thickness of the barrier was of 0.25 and 0.5 μm. Finally, highly doped ($N_D = 1 \times 10^{17}$ cm^{-3}) contact cap layer with a thickness of 1 μm and composition $x = x_{abs}$ was grown. In the n-N$^+$ junction is the x-graded region which represents the real structure which profile is shaped by interdiffusion processes during $Hg_{1-x}Cd_xTe$ growth at 350°C. The thickness of the gradient layer is about 0.3 μm. Thus, n$^+$/B/n/N$^+$ HgCdTe photodetector structure has been obtained as it is shown in Fig. 1. The thickness of the deposited layer was determined from the cleavage profile. Figure 2 presents the cleavage of HgCdTe layer grown on a 3-μm thick CdTe buffer layer.

The *n*- and *p*-type doping was achieved by *in-situ* doping with iodine and arsenic during horizontal, near atmospheric pressure MOCVD reactor with H_2 carrier gas, using the following precursors: di-isopropyl telluride (DiPTe), di-methyl cadmium (DMCd), and elemental mercury. An iodine precursor, *ethyl iodide* (EI), has been used for donor doping and it provides control over doping range from 10^{14} cm^{-3} to 1×10^{18} cm^{-3}. An arsenic precursor, tris-dimethylamino-arsenic (TDMAAs), has been used for acceptor doping and it provides control over doping concentration range between 10^{14} cm^{-3} and 5×10^{17}cm^{-3}.

The growth was carried out at temperatures of about 350°C and mercury zone at 210°C using the interdiffused multilayer process (IMP) technique on 2 inch, epiready, semi-insulating (100) GaAs substrates, oriented 2° off toward nearest <110>. Tellurium flush during nucleation process provides (111) CdTe growth. The II/VI mole ratio was kept in the range from 1.5 to 5 during CdTe cycles. About

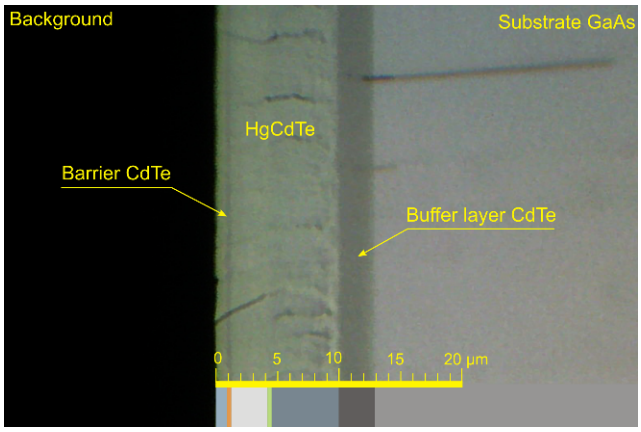

Fig. 2. Cleavage of a 10.5-μm thick detection layer grown on a 3-μm thick CdTe buffer layer.

3-μm thick CdTe layer was used as a buffer layer reducing stress caused by crystal lattice misfit between GaAs substrate and HgCdTe epitaxial layer structure. The growth was completed with cooling down procedure at metal rich ambient. No prolonged post growth dopant activation nor stoichiometric anneal was used. More comprehensive details of the growth experiments performed in our laboratory were published elsewhere [12,13].

Mesa-geometry structures were fabricated using wet etching to the highly doped bottom layer. Gold metal was deposited on the top and bottom contact layers. The electrical area of devices is 8.1×10^{-9} m^2.

3. Experimental results

The compositional and dopant profiles of the structure were controlled using secondary ion mass spectroscopy (SIMS). Figure 3 shows SIMS compositional and dopant profiles of typical MWIR n$^+$/B/n/N$^+$ structure measured by CAMECA IMS 6F using positive and negative Cs ions. The measured values of composition in the absorber region is consistent with the project. Undesired iodine presence in the absorber

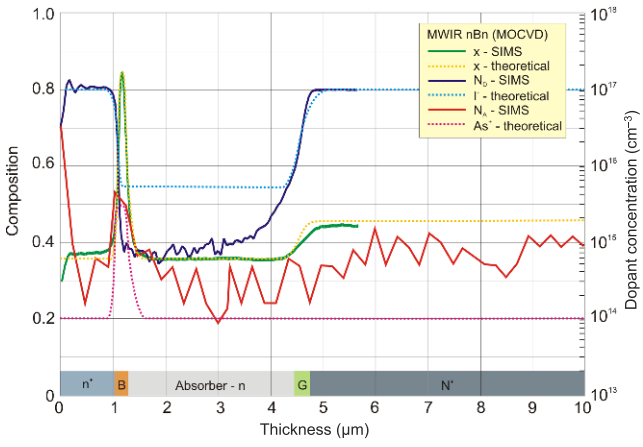

Fig. 3. SIMS measurements and theoretical assumption of composition and dopant profiles of typical MWIR n$^+$/B$_{(p)}$/n/N$^+$ structure.

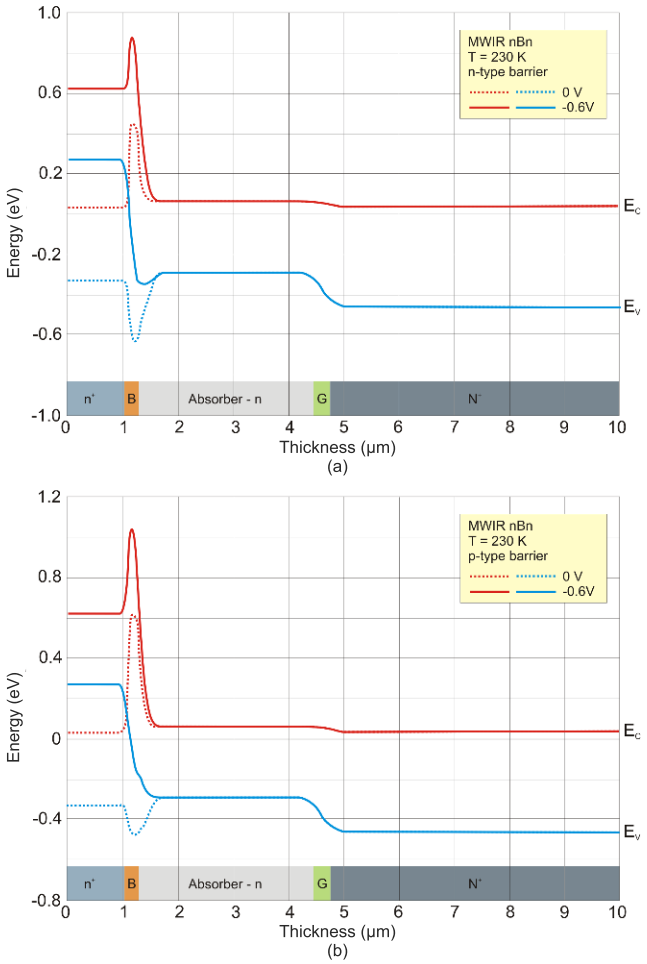

Fig. 4. Calculated energy band diagrams of the unbiased and 0.6 V reverse biased MWIR HgCdTe nBn photodetector operating at 230 K: (a) *n*-type barrier and (b) *p*-type barrier.

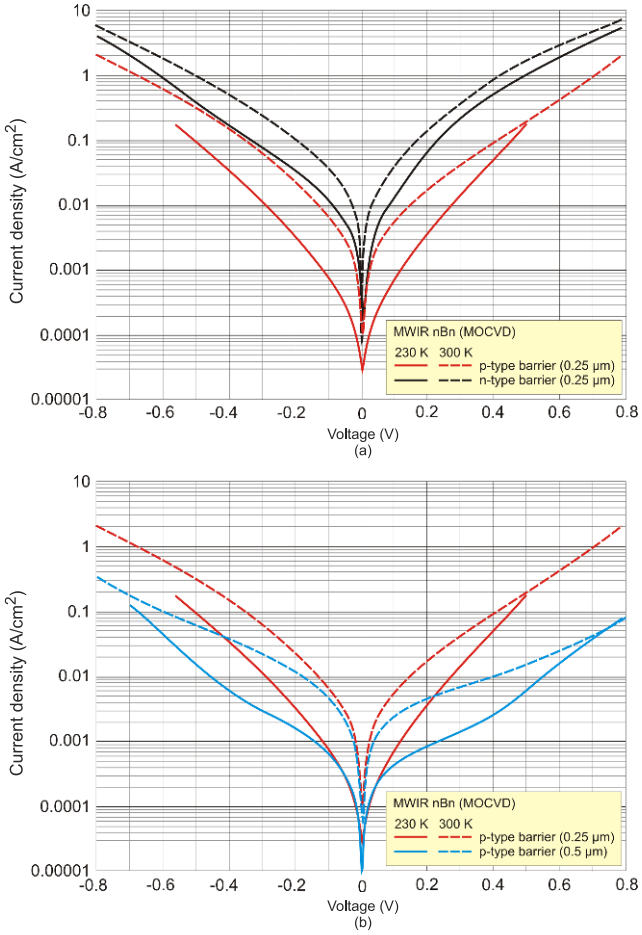

Fig. 5. Current-voltage characteristics of MWIR HgCdTe nBn photodetectors measured at 230 K and 300 K: (a) comparison for different barrier type and (b) comparison for different barrier thickness.

region is at the level of 1×10^{15} cm^{-3}, what is close to the SIMS detection sensitivity. The gradient slope of iodine line between n$^+$ and barrier region indicates iodine diffusion from n$^+$-region to the barrier what causes that the valance band offset increases. It strongly influences current densities of the devices. The dashed lines denote compositional and dopant profiles assumed on the basis of SIMS measurements and used for numerical analysis.

The assumed composition and doping concentration profiles presented in Fig. 3 permitted us to calculate the energy band diagrams for MWIR n$^+$/B/n/N$^+$ photodetectors (Fig. 4). The calculations have been performed for a device operating at 230 K using zero and the 0.6 V reverse bias voltage. The donor background concentration in the absorber region was assumed at the level of $N_D = 5 \times 10^{15}$ cm^{-3}. Under proper reverse bias, the holes are extracted from the absorber region by the negative electrode connected to the cap n$^+$ layer. The holes are also excluded from the absorber near the n-N$^+$ junction because they cannot be injected from the positive electrode into the bottom N$^+$ layer.

The current-voltage characteristics have been measured using the Keithley 2400 sourcemeter. The *I-V* characteristics of MWIR n$^+$/B/n/N$^+$ photodetector operating with Peltier cooling (solid lines) and room temperature (dashed lines) are presented in Fig. 5. Theoretically, the dark current of the n$^+$/B/n/N$^+$ device is expected to saturate under increasing reverse bias. However, it is difficult to control band offset in HgCdTe materials due to inherited "nested" band alignment. In steady state conditions, the interface of the wide band-gab barrier and the absorber region consist a valance band barrier blocking the flow of the minority carrier holes from the absorber (Fig. 4). Thus, holes accumulate in front of the barrier in the valence band causing increased thermal generation in the absorber region, which in turn increases the electron flow from the absorber to the N$^+$ bottom contact.

Figure 6 presents the current responsivity *vs*. wavelength for backside illuminated MWIR n$^+$/B/n/N$^+$ HgCdTe photodetectors measured at 230 K. The spectral characteristics have measured different reverse bias using the Perkin Elmer FT-IR Spectrometer type Spectrum 2000. Measured spectral response curves show a 3.6-μm cutoff wavelength

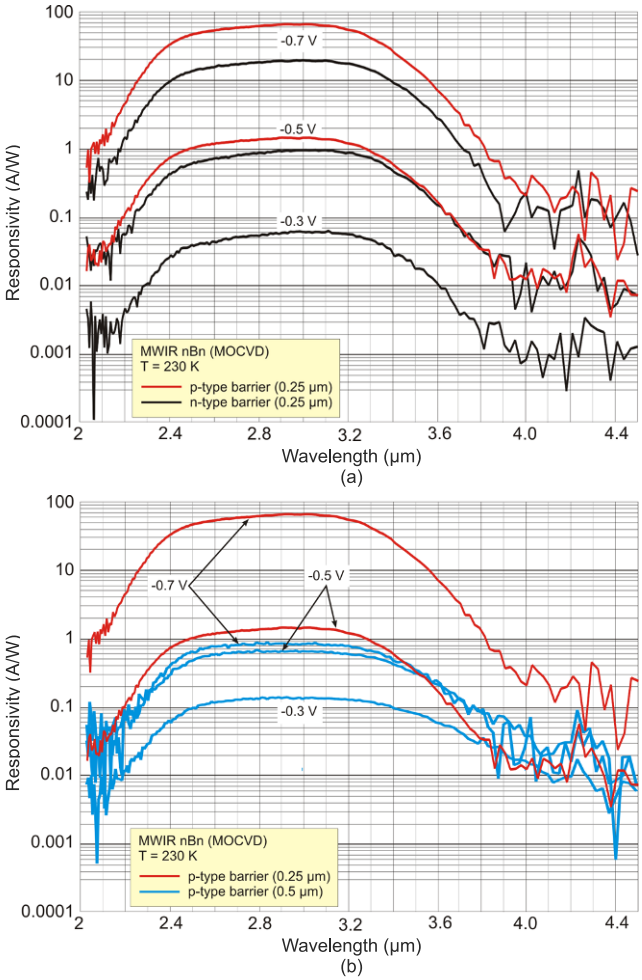

Fig. 6. Current responsivity *vs*. wavelength for MWIR HgCdTe nBn photodetectors measured at 230 K: (a) comparison for different barrier type and (b) comparison for different barrier thickness.

at 230 K. For devices with a 0.25-μm barrier thickness, the current responsivity increases when the reverse bias is applied. Appropriate reverse bias aligns the valance band and causes Auger-suppression. For devices with a barrier two times thicker, the current responsivity is two order of magnitude lower for 0.7 V, due to high resistance of the barrier.

4. Conclusions

In conclusion, this paper demonstrates the structure of $n^+/B/n/N^+$ HgCdTe detectors designed for the MWIR atmospheric window. The key item in limiting the performance of this structures is undesirable iodine diffusion from cap layer to the barrier what increase the valance band offset. However, the barrier architecture, integrated with Auger-suppression, might be a promising solution for high operating temperature infrared detectors grown by MOCVD. Further optimization of the $n^+/B/n/N^+$ structural parameters and processing steps are expected to improve the overall dark current density and response of the devices.

Since in the nBn structures the absorber is covered with the barrier which consists the passivation layer itself, the first test mesa-structures were not intentionally passivated. However, further study of devices with surface passivation is needed to determine the limiting dark current mechanisms.

Acknowledgement

The work has been done under the financial support of the Polish National Science Centre as research Project No. DEC-2011/03/D/ST7/03161.

References

1. C.T. Elliott, N.T. Gordon, R.S. Hall., T.J. Phillips, A.M. White, C.L. Jones *et al*., "Recent results on metaloorganic vapour phase epitaxially grown HgCdTe heterostructure devices", *J. Electron. Mater*. **25**, 1139–1145, 1996.
2. T. Ashley and C.T. Elliott, "Nonequilibrium devices for infra-red detection", *Electron. Lett*. **21**, 451–452, 1985.
3. T. Ashley, T.C. Elliott, and A.M. White, "Infra-red detector using minority carrier exclusion", *Proc SPIE* 572, 123–133, 1985.
4. J. Piotrowski, "$Hg_{1-x}Cd_xTe$ infrared photodetectors", In: *Infrared photon detectors* edited by A. Rogalski, Bellingham: SPIE Press, pp. 391–494, 1995.
5. J. Piotrowski and A. Rogalski, *High-Operating-Temperature Infrared Photodetectors*, Bellingham: SPIE Press, 2007.
6. S. Maimon and G. Wicks, "nBn detector, an infrared detector with reduced dark current and higher operating temperature," *Appl. Phys. Lett*. **89**, 151109 (2006).
7. P. Klipstein, "XBn' barrier photodetectors for high sensitivity and high operating temperature infrared sensors," *Proc. SPIE* **6940**, 69402U-1–11 (2008).
8. J.B. Rodriguez, E. Plis, G. Bishop, Y.D. Sharma, H. Kim, L.R. Dawson, and S. Krishna, "nBn structure based on InAs/GaSb type-II strained layer superlattices," *Appl. Phys. Lett*. **91**, 043514-1–2 (2007).
9. S. Velicu, J. Zhao, M. Morley, A.M. Itsuno, and J.D. Philips, "Theoretical investigation of MWIR HgCdTe nBn detectors," *Proc. SPIE* **8268**, 82682X (2012).
10. A.M. Itsuno, J.D. Philips, and S. Velicu, "Mid-wave infrared HgCdTe nBn photodetector," *Appl. Phys. Lett*. **100**, 161102 (2012).
11. A.M. Itsuno, J.D. Philips, and S. Velicu, "Design of an Auger-suppressed unipolar HgCdTe NBνN photodetector", *J. Electron. Mater*. **41**, 2886–2892 (2012).
12. P. Madejczyk, A. Piotrowski, W. Gawron, K. Kłos, J. Pawluczyk, J. Rutkowski, J. Piotrowski, and A. Rogalski,"Growth and properties of MOCVD HgCdTe epilayers on GaAs substrate", *Opto-Electron. Rev*. **13**, 239–251 (2005).
13. A. Piotrowski, P. Madejczyk, W. Gawron, K. Kłos, M. Romanis, M. Grudzień, J. Piotrowski, and A. Rogalski, "MOCVD growth of $Hg_{1-x}Cd_xTe$ heterostructures for uncooled infrared photodetectors", *Opto-Electron. Rev*. **12**, 453–458 (2004).